



Terrace width distributions for vicinal surfaces with steps of alternating stiffness

Jeremy A. Yancey ^{a,1}, Howard L. Richards ^{a,*}, T.L. Einstein ^b

^a Department of Physics, Texas A&M University-Commerce, Commerce, 2600 Neal Street, TX 75429-3011, United States

^b Department of Physics, University of Maryland, College Park, MD 20742-4111, United States

Received 31 May 2005; accepted for publication 30 August 2005

Available online 21 October 2005

Abstract

For the typical elastic interactions between steps, the generalized Wigner distribution (GWD) has been shown to be in excellent quantitative agreement with terrace width distributions (TWDs) calculated from numerical simulations. Here we show that the TWDs of vicinal surfaces with steps of alternating stiffness (but the same sort of step–step repulsions) are also given by the GWD. In the key parameter, the dimensionless repulsion strength, the step stiffness is generalized to twice the “reduced stiffness” of the two kinds of steps, as befits the inertial nature of stiffness. These results should also be applicable to more general surfaces with steps of different stiffness.

© 2005 Elsevier B.V. All rights reserved.

Keywords: Equilibrium thermodynamics and statistical mechanics; Stepped single crystal surfaces; Surface structure, morphology, roughness and topography; Surface energy; Vicinal single crystal surfaces

1. Introduction

When a crystal is cleaved at a small angle to a high-symmetry direction (corresponding to small Miller indices), the newly exposed surface is often

composed of terraces of the high-symmetry surface separated by steps of one or a few atoms in height [1]. The lower coordination number of surface atoms can lead to relaxations [1–9], in atomic position, reconstruction [1,2,7,10–13] of the surface into a different order, and the creation of new electronic states not present in the bulk material [14,15]. Such a vicinal, or stepped, surface can be exploited for use in catalysts [10,11,16], or for growing structures such as quantum wires and other electronic components [17], as well as for basic scientific research.

* Corresponding author. Tel.: +1 903 886 5882/5487; fax: +1 903 886 5480.

E-mail address: Howard_Richards@tamu-commerce.edu (H.L. Richards).

¹ Present address: Department of Physics and Astronomy, P.O. Drawer 5167, Mississippi State, MS 39762-5167, United States.

The relaxations, reconstructions, and surface electronic states give rise to effective interactions between steps, which obviously can be quite complicated in general. In most cases, though, the interactions between two neighboring steps are believed to be approximately described by the potential [1,13,18].

$$V(L) = \frac{A}{L^2}, \tag{1}$$

where A is an interaction constant and L is the width of the terrace (see Fig. 1). This potential is the dominant term in an expansion of the elastic interactions, and Eq. (1) is considered by most researchers in the field to sufficiently describe all step–step interactions.

Although the interaction between steps has been calculated for a few model surfaces, the elastic interactions require large numbers of atoms to be included in the calculations, which makes them computationally demanding. (See, e.g. Refs. [8,9].) Furthermore, the results are somewhat dependent on approximations used to simplify the quantum-mechanical treatment of electrons. A more practical method for determining fundamental parameters, such as the interaction constant A and the kink energy ϵ , is to infer them from experimental measurements of statistical properties, such as the terrace width distribution [19,20] (TWD) and

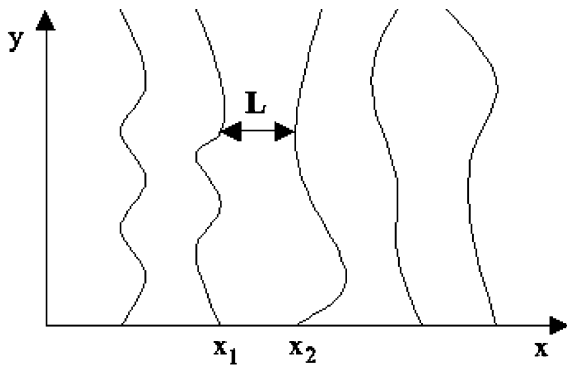


Fig. 1. Steps can be mapped onto the world-lines of spinless fermions. The average direction of the steps (y in “Maryland notation”) maps onto (imaginary) time. L is the width of the terrace between the steps at x_1 and x_2 .

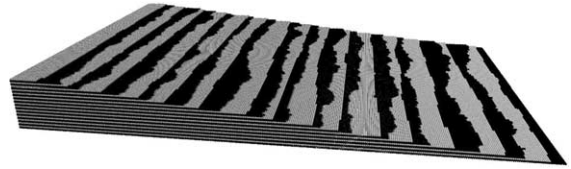


Fig. 2. TSK model of an AB-type vicinal crystal surface. The stiffness of steps with light terraces to the left is greater than the stiffness of the steps with dark terraces to the right. In this illustration, there is no interaction between the steps ($\vec{A} = 0$), and the stiffness ratio is $R = 8$.

wandering function [19,21], $\langle [x_i(y + \Delta y) - x_i(y)]^2 \rangle$, which is related to spatial autocorrelations.

The organization of this paper is as follows [22]. In Section 2 we review some approximations for TWDs for vicinal surfaces with steps all of the same stiffness. In Section 3, we extend the discussion of Section 2 to cover the case in which the steps do not all have the same stiffness, with particular attention to the case in which two types of steps alternate (Fig. 2). Silicon surfaces vicinal to the (100) plane are perhaps the most important example of such surfaces. (For a review of stepped Si surfaces, see Ref. [23].) Another realization is a surface vicinal to the basal plane of an hcp crystal in a principal direction such that the step edges are close-packed. A vicinal surface with metallic decoration on the lower side of each step, as for [wide] quantum wires, could also exhibit such properties. In this first attack on the problem, we neglect the possibility that the alternating stiffnesses may well be associated with alternating stress domains that can lead to more complicated interactions between steps [24]. Section 4 shows that TWDs derived from Monte-Carlo simulations of the Terrace-Step-Kink (TSK) model are in agreement with the predictions of Section 3. We summarize and conclude with a discussion of the relevance of this work to more complicated systems, such as vicinal surfaces of superlattices, in Section 5.

2. Approximate hamiltonians and terrace width distributions

When the step–step interactions are described by Eq. (1), the static properties of a system of

two steps with identical stiffness rely only on a single dimensionless parameter \tilde{A} , called the dimensionless interaction strength, which is defined as

$$\tilde{A} \equiv \frac{\tilde{\beta}A}{(k_B T)^2}, \quad (2)$$

where $\tilde{\beta}$ is the step stiffness, k_B is Boltzmann's constant, and T is the temperature.

Following the lead of Feynman [25], we can express the expectation values of the step position by mapping the statistical mechanical problem in two dimensions into a quantum mechanical problem in one dimension, with $k_B T$ taking the place of \hbar , $\tilde{\beta}$ taking the place of mass, and the average direction of the steps (the y -direction) being interpreted as imaginary time [26–28].

The TWD can then be found by making a Gruber–Mullins [19,29] approximation, in which one step fluctuates freely but its neighbors are held straight and fixed. The probability of the fluctuating step being at position x is given in the usual fashion from the ground state,

$$P(x) = |\psi_0(x)|^2, \quad (3)$$

of the Schrödinger equation

$$\begin{aligned} & \left\{ \frac{\mathcal{H}_{\text{GM}} - E_n}{a} \right\} \psi_n(x) \\ & \equiv \left\{ -\frac{(k_B T)^2}{2\tilde{\beta}} \frac{d^2}{dx^2} + U_{\text{GM}}(x) - \frac{E_n}{a} \right\} \psi_n(x) = 0, \end{aligned} \quad (4)$$

where $U_{\text{GM}}(x)$ is a “confining potential” due to the fixed neighboring steps. (The factors a^{-1} is due to the fact that energies have to be measured per unit length along the y -direction.) This approximation is useful only for strong repulsions between steps, in which case

$$\begin{aligned} U_{\text{GM}}(x) & \equiv V(x) + V(2\langle L \rangle - x) - 2V(\langle L \rangle) \\ & \approx \frac{6A}{\langle L \rangle^4} (x - \langle L \rangle)^2, \end{aligned} \quad (5)$$

where $\langle L \rangle$ is the average distance between steps. The resulting TWD is a Gaussian, which is in qualitative agreement with experimental observations.

However, even in the limit of strong repulsions, the variance of this Gaussian approximation does not match the variance of TWDs obtained from simulations as well as might be desired [30,31]. At weak or moderate repulsions, TWDs from simulations and experiments show noticeable asymmetry, and the Gaussian approximation clearly fails.

This approximation can be greatly improved by (1) explicitly considering the fluctuations and interactions of *two adjacent* steps and by (2) relaxing the condition that the steps neighboring them on either side be fixed in position. This approximation yields a Schrödinger equation of the form [32].

$$\begin{aligned} & \left\{ \frac{H - E_n}{a} \right\} \Psi_{n,m}(x_1, x_2) \\ & \equiv \left\{ -\frac{(k_B T)^2}{2\tilde{\beta}} \left[\frac{\partial^2}{\partial x_1^2} + \frac{\partial^2}{\partial x_2^2} \right] + V(x_2 - x_1) \right. \\ & \quad \left. + U(x_1, x_2) - \frac{E_{n,m}}{a} \right\} \Psi_{n,m}(x_1, x_2) = 0. \end{aligned} \quad (6)$$

The confining potential can be related to the pressure and compressibility of the steps through a phenomenological argument, but in the case of repulsive interactions following Eq. (1), it can be taken to be of the form:

$$U(x_1, x_2) = \frac{U_2}{2} (x_1^2 + x_2^2), \quad (7)$$

where U_2 is chosen to produce the correct average terrace width, $\langle L \rangle \equiv \langle x_2 - x_1 \rangle$. Eq. (6) is then separable, so that $\Psi_{n,m}(x_1, x_2) = \psi_n(x_2 - x_1)\phi_m(x_1 + x_2)$, and Eq. (3) can again be used to determine the TWD. The resulting terrace width distribution is the “generalized Wigner distribution”.

In terms of the normalized terrace width [33],

$$s \equiv \frac{L}{\langle L \rangle}, \quad (8)$$

the generalized Wigner distribution (GWD) is given by [34–36]

$$P_\rho(s) = a_\rho s^\rho \exp(-b_\rho s^2). \quad (9)$$

Here

$$\rho \equiv 1 + \sqrt{1 + 4\tilde{A}}. \quad (10)$$

The requirement $\langle s \rangle \equiv \langle L / \langle L \rangle \rangle = 1$ yields

$$b_\rho \equiv \left[\frac{\Gamma(\frac{\rho+2}{2})}{\Gamma(\frac{\rho+1}{2})} \right]^2 \tag{11}$$

and normalization yields

$$a_\rho \equiv \frac{2b_\rho^{(\rho+1)/2}}{\Gamma(\frac{\rho+1}{2})}. \tag{12}$$

The generalized Wigner distribution has been shown to be in excellent quantitative agreement with TWDs derived from Monte-Carlo simulations of the TSK model and in qualitative agreement with many experimentally measured TWDs [20,30,36–38]. In particular, over the most physically relevant range of \tilde{A} (from 0 to about 12), the GWD is in better agreement with TWDs from simulations than even improved versions [31,39–43] of the Gaussian approximation [30].

The small discrepancies between the GWD and simulation results can be best understood when one realizes that the GWD is the *exact* solution of an eigenproblem (Eq. (6)) which is itself the result of three approximations, which are practically unavoidable.

1. The atomically discrete steps are coarse-grained into gently varying continuous curves [44] in order to apply results from capillary wave theory. Obviously, this approximation becomes problematic when $\langle L \rangle$ is small, e.g. $\langle L \rangle < 5a$ [20]. Eq. (6) assumes that terms of order $\mathcal{O}(\theta^3)$ and higher, where θ is the angle of the step with the y -direction, can safely be ignored in the Taylor series expansion of the free energy of the step (per unit length). At high temperatures, the steps are not “gently varying”, so this assumption fails, and the GWD describes the TWD less well [19,30].
2. The TWD is determined from a pure quantum state involving only two steps explicitly. Due to interactions with the other steps, a density matrix should be used rather than a pure quantum state [45].
3. The confining potential defined by Eq. (7) has only one adjustable parameter, U_2 , which is *entirely determined by the mean step separation, $\langle L \rangle$* . As a result, if the interaction between steps

is of the form $A/(x_i - x_j)^2$, the GWD can have no dependence on whether j is restricted to $i \pm 1$ (neighboring steps) or to all $j \neq i$. This is the origin of the “remarkable and curious” insensitivity of the GWD to the range of step-step interactions mentioned in Ref. [30]. It should be possible to account for the small dependence on the range of interaction that is observed in Monte-Carlo TWDs by giving $U(x_1, x_2)$ a more general form than Eq. (7); the most justifiable extensions, however, would spoil the separability of the Hamiltonian and prevent simple, analytic solutions.

In spite of the intimidating presence of gamma functions in Eqs. (11) and (12), the GWD is just as easy to apply to experimental data as the Gaussian approximation. From the experimental TWD, $P_{\text{exp}}(L)$, can be calculated both the mean terrace width,

$$\langle L \rangle_{\text{exp}} \equiv \sum_L P_{\text{exp}}(L)L \tag{13}$$

and the variance,

$$\sigma_{\text{exp}}^2 \equiv \sum_L P_{\text{exp}}(L)(L - \langle L \rangle_{\text{exp}})^2. \tag{14}$$

These in turn can be used to estimate the dimensionless interaction constant \tilde{A} from the approximation

$$\tilde{A} \approx \frac{1}{16} \left[\left(\frac{\sigma_{\text{exp}}^2}{\langle L \rangle_{\text{exp}}^2} \right)^{-2} - 7 \left(\frac{\sigma_{\text{exp}}^2}{\langle L \rangle_{\text{exp}}^2} \right)^{-1} + \frac{27}{4} + \frac{35}{6} \left(\frac{\sigma_{\text{exp}}^2}{\langle L \rangle_{\text{exp}}^2} \right) \right]. \tag{15}$$

Note that other estimates of $\langle L \rangle$ not calculated directly from $P_{\text{exp}}(L)$, e.g. calculated from the nominal angle of miscut, often differ from $\langle L \rangle_{\text{exp}}$ by 5–10%, which can cause significant errors in the extracted value of \tilde{A} .

3. Theoretical derivation of the generalized Wigner distribution

In this section we consider a vicinal surface in which the odd-numbered steps have stiffness $\tilde{\beta}_1$ and the even-numbered steps have stiffness $\tilde{\beta}_2$. If

$V(L)$ is given by Eq. (1), we will show that the TWD is given by a generalized Wigner distribution. In consequence, the results discussed at the end of the previous section apply, in particular the use of Eq. (15) to extract the dimensionless interaction constant \tilde{A} . This section generalizes parallel arguments in Section IIB of Ref. [32], where all steps had the same stiffness.

Generalizing from Eq. (6), the Hamiltonian of two neighboring steps with positions x_1 and x_2 is

$$\frac{H}{a} \equiv -\frac{(k_B T)^2}{2} \left(\frac{1}{\beta_1} \frac{\partial^2}{\partial x_1^2} + \frac{1}{\beta_2} \frac{\partial^2}{\partial x_2^2} \right) + V(x_2 - x_1) + U(x_1, x_2), \quad (16)$$

where V the step–step interaction potential and U is the confining potential for a pair of steps.

As in Ref. [32], the form of $U(x_1, x_2)$ is justified by a phenomenological argument, which begins with an analogy. The motion of a polymer in a polymer melt is constrained by a reptation tube [46,47]. The constraint is not truly fixed, but *on the time scale of the mean collision time* it is *practically* fixed. On longer time scales, the polymer may nevertheless diffuse over any distance.

Likewise, the neighborhood of a pair of adjacent steps constrains the wanderings of those steps. Over a distance in the y -direction on the scale of the “step collision distance” or correlation length, the pair are not sensitive to the size of the system in the x -direction beyond some limit, so we may consider the pair to be confined in a “box” of that size. $U(x_1, x_2)$ can then be calculated from thermodynamic considerations. This approach works well for TWDs, since they involve differences in x -coordinates at *the same* y -coordinate, but caution is required when applying it to functions like the step wandering function that involve differences in x -coordinates at *different* y -coordinates. As with the polymer above, the step pair may eventually diffuse over any distance.

The above approach is implemented as follows. The step at x_1 is taken to be the right wall of a box containing $\mathcal{V}/\langle L \rangle$ steps with a fixed left wall at $x = -\mathcal{V}$, so the volume (length) of this box is $\mathcal{V}_1 = \mathcal{V} + x_1$. A Taylor expansion of the pressure term for this step yields

$$\begin{aligned} \mathcal{P}_1(x_1) &= \mathcal{P} + x_1 \left(\frac{\partial \mathcal{P}_1}{\partial x_1} \right) \Big|_{x_1=0} + \mathcal{O}(x_1^2) \\ &= \mathcal{P} + x_1 \left(\frac{\partial \mathcal{P}_1}{\partial \mathcal{V}_1} \right) \Big|_{\mathcal{V}_1=\mathcal{V}} + \mathcal{O}(x_1^2) \\ &= \mathcal{P} - x_1 (\mathcal{V} \kappa)^{-1} + \mathcal{O}(x_1^2), \end{aligned} \quad (17)$$

where $\mathcal{P} \equiv \mathcal{P}_1(0)$, and the isothermal compressibility κ is given by [48]

$$\kappa \equiv -\frac{1}{\mathcal{V}} \left(\frac{\partial \mathcal{P}_1}{\partial \mathcal{V}_1} \right)^{-1} \Big|_{\mathcal{V}_1=\mathcal{V}}. \quad (18)$$

Likewise, the step at x_2 is the left wall of a box containing $\mathcal{V}/\langle L \rangle$ steps with a fixed right wall at $x = +\mathcal{V}$, the volume (length) of this box is $\mathcal{V}_2 = \mathcal{V} - x_2$ and the expansion of the pressure term for this step is

$$\mathcal{P}_2(x_2) = \mathcal{P} + x_2 (\mathcal{V} \kappa)^{-1} + \mathcal{O}(x_2^2) \quad (19)$$

Using the Taylor expansions from Eqs. (17) and (19) for the pressure exerted on the steps at x_1 and x_2 , the confining potential can be written in the following way:

$$\begin{aligned} U(x_1, x_2) &= -x_1 \mathcal{P}_1(x_1) + x_2 \mathcal{P}_2(x_2) \\ &= (x_2 - x_1) \mathcal{P} + (x_1^2 + x_2^2) (\mathcal{V} \kappa)^{-1} \\ &\quad + \mathcal{O}(x_2^3 - x_1^3). \end{aligned} \quad (20)$$

Mindful of the transformation [49] between the coordinates of two interacting particles and the coordinates of their center of mass and relative separation, we introduce the linear canonical transformation given by

$$\begin{aligned} L &= x_2 - x_1 \geq 0, \\ z &= c_1 x_1 + c_2 x_2, \end{aligned} \quad (21)$$

where c_1 and c_2 are arbitrary constants to be determined later and L is the terrace width between the two steps. With this transformation, the Hamiltonian in Eq. (16) becomes

$$\begin{aligned} \frac{\mathcal{H}}{a} &= -\frac{(k_B T)^2}{2} \left\{ \frac{1}{\beta_r} \frac{\partial^2}{\partial L^2} + 2 \left(\frac{c_2}{\beta_2} - \frac{c_1}{\beta_1} \right) \frac{\partial^2}{\partial L \partial z} \right. \\ &\quad \left. + \left(\frac{c_1^2}{\beta_1} + \frac{c_2^2}{\beta_2} \right) \frac{\partial^2}{\partial z^2} \right\} + V(L) + U(L, z), \end{aligned} \quad (22)$$

where

$$\tilde{\beta}_r \equiv \frac{\tilde{\beta}_1 \tilde{\beta}_2}{\tilde{\beta}_1 + \tilde{\beta}_2} \quad (23)$$

is the “reduced stiffness” of the two steps, analogous to their reduced mass (consistent with the analogy of stiffness to mass in our model).

Since the constants c_1 and c_2 are arbitrary, we can choose them so that the cross-differentiation term vanishes; that is,

$$c_1 = \frac{\tilde{\beta}_r}{\tilde{\beta}_2} = \frac{\tilde{\beta}_1}{\tilde{\beta}_1 + \tilde{\beta}_2} \quad (24)$$

and

$$c_2 = \frac{\tilde{\beta}_r}{\tilde{\beta}_1} = \frac{\tilde{\beta}_2}{\tilde{\beta}_1 + \tilde{\beta}_2}, \quad (25)$$

which, in turn, make z analogous to the center of mass of the two steps:

$$z = \frac{\tilde{\beta}_1 x_1 + \tilde{\beta}_2 x_2}{\tilde{\beta}_1 + \tilde{\beta}_2}. \quad (26)$$

Using this specification of z , the Hamiltonian of Eq. (16) has a “nearly” separable form:

$$\begin{aligned} \mathcal{H} = \mathcal{H}_L + \mathcal{H}_z - \frac{a}{\mathcal{V}\kappa} \left(\frac{\tilde{\beta}_1 - \tilde{\beta}_2}{\tilde{\beta}_{\text{avg}}} \right) zL + \mathcal{O}(z^3) \\ + \mathcal{O}(z^2L) + \mathcal{O}(zL^2) + \mathcal{O}(L^3), \end{aligned} \quad (27)$$

where

$$\begin{aligned} \frac{\mathcal{H}_L}{a} \equiv -\frac{(k_B T)^2}{2\tilde{\beta}_r} \frac{\partial^2}{\partial L^2} + V(L) + \mathcal{P}L + \frac{1}{\mathcal{V}\kappa} \left(1 - \frac{\tilde{\beta}_r}{\tilde{\beta}_{\text{avg}}} \right) L^2, \\ \frac{\mathcal{H}_z}{a} \equiv -\frac{(k_B T)^2}{4\tilde{\beta}_{\text{avg}}} \frac{\partial^2}{\partial z^2} + \frac{2}{\mathcal{V}\kappa} z^2, \end{aligned} \quad (28)$$

give the primary L and z -dependent portions of the Hamiltonian, and

$$\tilde{\beta}_{\text{avg}} \equiv \frac{\tilde{\beta}_1 + \tilde{\beta}_2}{2} \quad (29)$$

is the average stiffness of the step pair. Notice that when the steps have the same stiffness, the zL cross-term in Eq. (27) vanishes, leaving the separable Hamiltonian considered in Ref. [32] when higher-order terms are neglected.

In order to use separation of variables to solve the Schrödinger equation, we neglect the zL cross-term. The assumption that the zL term can be eliminated from the Hamiltonian along with the other higher order terms is vindicated in the next section, in the sense that the square of the resulting ground state solution gives remarkably good agreement with TWDs from numerical simulations, even when the ratio of stiffnesses is unphysically large.

Due to separation of variables, the two-step Hamiltonian reduces to an ordinary differential equation in z and an ordinary differential equation in L . The latter is given by

$$\begin{aligned} \left\{ \frac{\mathcal{H}_L - E_L}{a} \right\} \psi(L) = \left[-\frac{(k_B T)^2}{2\tilde{\beta}_r} \frac{d^2}{dL^2} + V(L) + \mathcal{P}L \right. \\ \left. + \frac{1}{\mathcal{V}\kappa} \left(1 - \frac{\tilde{\beta}_r}{\tilde{\beta}_{\text{avg}}} \right) L^2 - \frac{E_L}{a} \right] \psi(L) \\ = 0, \end{aligned} \quad (30)$$

where the L subscript on the energy E_L is intended only to remind the reader that this is the portion of the total energy associated with the variable L and not with z . (To avoid confusion, we suppress the index n indicating the eigenfunction/eigenvalue pair.) For simplicity, we rewrite Eq. (30), solving for the doubly differentiated term:

$$\begin{aligned} \frac{d^2 \psi(L)}{dL^2} = \frac{2\tilde{\beta}_r}{(k_B T)^2} [V(L) + \mathcal{P}L \\ + \frac{1}{\mathcal{V}\kappa} \left(1 - \frac{\tilde{\beta}_r}{\tilde{\beta}_{\text{avg}}} \right) L^2 - \frac{E_L}{a}] \psi(L). \end{aligned}$$

The substitutions,

$$\begin{aligned} \tilde{U}(L) &\equiv \frac{2\tilde{\beta}_r}{(k_B T)^2} U(L) \langle L \rangle^2 \\ &= \frac{2\tilde{\beta}_r}{(k_B T)^2} \left[\mathcal{P}L + \frac{1}{\mathcal{V}\kappa} \left(1 - \frac{\tilde{\beta}_r}{\tilde{\beta}_{\text{avg}}} \right) L^2 \right] \langle L \rangle^2, \end{aligned}$$

$$\tilde{E}_L \equiv \frac{2\tilde{\beta}_r}{(k_B T)^2} \frac{E_L}{a} \langle L \rangle^2,$$

and use of Eq. (8) lead to the dimensionless form of the Schrödinger equation:

$$\frac{d^2 \psi(s)}{ds^2} = [\tilde{V}(s) + \tilde{U}(s) - \tilde{E}_L] \psi(s). \quad (31)$$

So far, only one assumption has been made as to the nature of the step–step interaction—that it is a function of the step separation. If, however, the interaction is of the form given in Eq. (1), it is given in dimensionless form by

$$\tilde{V}(s) = \frac{\tilde{A}}{s^2}. \quad (32)$$

The dimensionless interaction \tilde{A} is dependent on an effective step stiffness, $\tilde{\beta}_{\text{eff}}$, equal to twice the reduced stiffness:

$$\tilde{A} \equiv \frac{\tilde{\beta}_{\text{eff}} A}{(k_{\text{B}} T)^2}, \quad (33)$$

$$\tilde{\beta}_{\text{eff}} = 2\tilde{\beta}_r = \frac{2\tilde{\beta}_1 \tilde{\beta}_2}{\tilde{\beta}_1 + \tilde{\beta}_2}, \quad (34)$$

instead of the definition used for steps of the same stiffness (Eq. (2)). Note that, if $\tilde{\beta}_1 = \tilde{\beta}_2 = \tilde{\beta}$, then $\tilde{\beta}_{\text{eff}} = 2\tilde{\beta}_r = \tilde{\beta}$, and Eq. (33) reverts to Eq. (2), giving the familiar dimensionless step–step interaction and its corresponding step–step interaction potential (Eq. (1)).

To make further progress, we assume that $(\mathcal{V}\kappa)_{-1} \gg \mathcal{P}$ in Eq. (31), so that we can neglect the linear term in the confining potential as was done in Ref. [32]. With this assumption, the Schrödinger equation simplifies to the analytically solvable form:

$$\frac{d^2\psi(s)}{ds^2} = \left[\frac{\tilde{A}}{s^2} + \Omega^2 s^2 - \tilde{E}_L \right] \psi(s), \quad (35)$$

where

$$\Omega^2 \equiv \frac{\tilde{A}}{A} \left(1 - \frac{\tilde{\beta}_r}{\tilde{\beta}_{\text{avg}}} \right) \frac{\langle L \rangle^4}{\mathcal{V}\kappa}$$

is some dimensionless constant. The ground state eigenfunction for the case of alternating stiffness is thus

$$\psi_0(s) = c_0 s^{\frac{L}{2}} \exp\left(-\frac{1}{2} b_\rho s^2\right), \quad (36)$$

where the requirement $\langle s \rangle \equiv \langle L / \langle L \rangle \rangle = 1$ yields

$$\Omega^2 = b_\rho, \quad (37)$$

and normalization yields

$$c_0^2 = a_\rho. \quad (38)$$

Squaring the modulus of this state to find the TWD, we obtain the generalized Wigner distribution as given in Eq. (9).

4. Comparison with simulations of the TSK model

In this section we use Monte-Carlo simulations of the TSK model to test the prediction, made in the previous section, that the GWD is also a good approximation for the TWDs of surfaces with steps of alternating stiffness.

The system of alternating steps was modeled using the TSK Hamiltonian, with kink energies given by

$$\begin{aligned} \varepsilon_{2n+1} = \varepsilon_1 &\equiv 2k_{\text{B}} T \sinh^{-1} \left(\sqrt{\frac{R+1}{2R}} \sinh \left(\frac{\varepsilon_0}{2k_{\text{B}} T} \right) \right), \\ \varepsilon_{2n} = \varepsilon_2 &\equiv 2k_{\text{B}} T \sinh^{-1} \left(\sqrt{\frac{R+1}{2}} \sinh \left(\frac{\varepsilon_0}{2k_{\text{B}} T} \right) \right), \end{aligned} \quad (39)$$

where n is an integer and

$$R = \frac{\tilde{\beta}_{2n}}{\tilde{\beta}_{2n+1}} = \frac{\tilde{\beta}_2}{\tilde{\beta}_1} \quad (40)$$

is the stiffness ratio of the even to the odd numbered steps. The rather arcane formula for kink energies given by Eq. (39) is chosen so that, when these kink energies are used to calculate the stiffness of each step [21], the values of $\tilde{\beta}_i$ are conveniently related:

$$\begin{aligned} \tilde{\beta}_{2n+1} = \tilde{\beta}_1 &= \frac{2k_{\text{B}} T}{a} \sinh^2 \left(\frac{\varepsilon_1}{2k_{\text{B}} T} \right) \\ &= \left(\frac{R+1}{R} \right) \frac{k_{\text{B}} T}{a} \sinh^2 \left(\frac{\varepsilon_0}{2k_{\text{B}} T} \right), \end{aligned} \quad (41)$$

$$\begin{aligned} \tilde{\beta}_{2n} = \tilde{\beta}_2 &= \frac{2k_{\text{B}} T}{a} \sinh^2 \left(\frac{\varepsilon_2}{2k_{\text{B}} T} \right) \\ &= (R+1) \frac{k_{\text{B}} T}{a} \sinh^2 \left(\frac{\varepsilon_0}{2k_{\text{B}} T} \right). \end{aligned}$$

Thus, the choice of the kink energies in Eq. (39) insures that the effective stiffness of Eq. (33) remains constant when the stiffness ratio is varied:

$$\tilde{\beta}_{\text{eff}} = \frac{2\tilde{\beta}_1\tilde{\beta}_2}{\tilde{\beta}_1 + \tilde{\beta}_2} = \frac{2}{R + 1}$$

$$\tilde{\beta}_2 = \frac{2k_B T}{a} \sinh^2\left(\frac{\varepsilon_0}{2k_B T}\right). \quad (42)$$

The temperature of each simulated system was related to the kink energies of the steps using the relation $k_B T = 0.45\varepsilon_0$. The resulting effective step stiffness is about $1.65\varepsilon_0/a$. Each simulated system had 30 steps, 15 of which had kink energy ε_1 and 15 of which had ε_2 . Each step was $1000a$ in length with a mean step separation of $10a$, and periodic boundary conditions were applied in both the x - and y -directions; the lattice spacing a is the unit of length.

A single-site Metropolis algorithm [50] was used for the simulations. Each simulation was equilibrated for at least 10^6 Monte-Carlo steps per site (MCSS). ‘‘Snapshots’’ (complete records of step positions) were recorded at intervals of 10^3 MCSS, for a total of 10^3 snapshots. A TWD was calculated for each snapshot; these were averaged together, and error bars were calculated using the bootstrap method [51,52].

Simulations were run with $\tilde{A} = 0, 2, 4, 6, 8$, and 10 ; for each value of \tilde{A} , simulations were run $R = 1, 2, 4$, and 8 . The plots shown in Fig. 3 demonstrate the agreement between the terrace width distributions generated from Monte-Carlo TSK simulations and the generalized Wigner distribution. Fig. 3(a), for example, shows the TSK simulation data for the four $\tilde{A} = 0$. Simulation results are plotted as symbols, whereas the GWD is shown by the solid curve. Error bars are much smaller than the symbol size. Very good agreement is observed between the simulation data and the GWD. Some tendency for larger values of R to produce slightly sharper TWDs is observed.

It is important to understand that the simulations presented in this section are only intended as illustrations of a generic surface with steps of alternating stiffness; they are not meant as detailed models of any particular experimental system. The simulation temperature $k_B T = 0.45\varepsilon_0$ was chosen as a compromise: if the temperature is too low, the Monte-Carlo algorithm becomes inefficient,

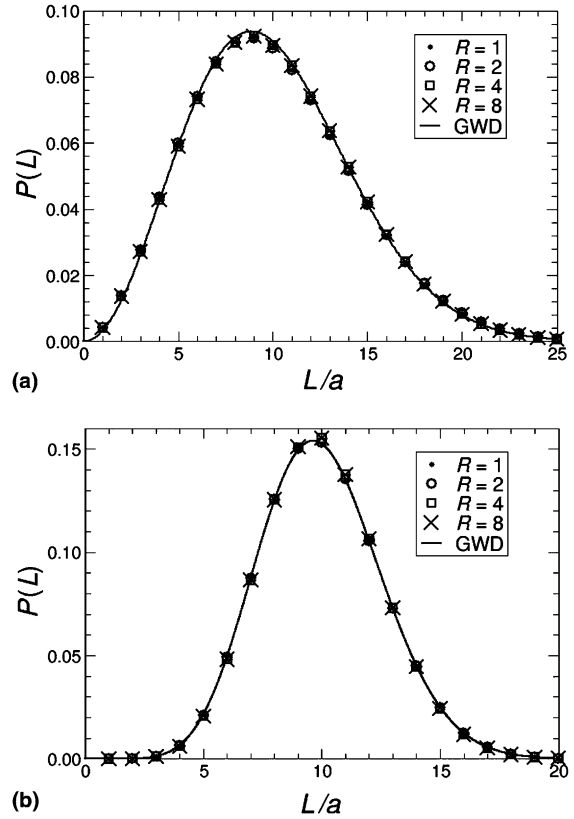


Fig. 3. Comparison of the generalized Wigner distribution (GWD) with Monte-Carlo simulation data for various step stiffness ratios (R). Plot (a) shows the TWDs for dimensionless step-step interactions of $\tilde{A} = 0$; (b) is for $\tilde{A} = 10$. Comparisons for $\tilde{A} = 2, 4, 6$, and 8 (not shown) show similar agreement.

but if the temperature is too high, the steps are not ‘‘gently varying’’, so the GWD describes the TWD less well, as was mentioned earlier. This same consideration discourages the simulation of large stiffness ratios, since as R becomes large, $k_B T/\varepsilon_1$ becomes larger and $k_B T/\varepsilon_2$ becomes smaller.

It is likewise worth emphasizing that even when good experimental estimates exist for the kink energies, as is the case for Si(001) [53–55], they should not be naively substituted into Eq. (41). Only if there are no interactions or correlations between kinks will Eq. (41) be valid. However, it has been shown that correlations between kinks cannot be ignored for Ge(001) vicinal surfaces [56].

5. Discussion

We have shown that the terrace width distributions depend only weakly on the stiffness ratio, so long as the dimensionless interaction constant \tilde{A} is correctly calculated using the effective step stiffness given in Eq. (34). The neglected terms of Eq. (27) are not numerically significant for physically reasonable interaction strengths and step stiffness ratios. This result extends the utility of the generalized Wigner distribution to a greater variety of vicinal surfaces.

The most serious simplification we have made is, without doubt, the assumption that the interaction is the same between both species of steps. To facilitate discussion, let us say that a step of type S_β^α separates a terrace of type T_α (above) and a terrace of type T_β (below), etc. A silicon surface vicinal to the (001) plane would thus consist of terrace of types T_α and T_β (representing different orientations of the dimers with respect to the step direction) in strict alternation, separated alternately by steps of types S_β^α and S_α^β .

There is no reason to expect that in real materials the step–step interaction potential will be independent of the type of terrace separating the steps. In the case of Si(100), it may be anticipated that there will be some difference depending on whether the dimers are oriented parallel or perpendicular to the steps, even though both terraces have (in the limit of wide terraces) the same surface free energy density. For other surfaces the effects may be more dramatic. Because the interaction $V_\alpha(L_\alpha)$ across a T_α terrace is different from the interaction $V_\beta(L_\beta)$ across a T_β terrace, the corresponding average terrace widths, $\langle L_\alpha \rangle$ and $\langle L_\beta \rangle$, are different, as are the corresponding TWDs. Nevertheless, as long as $\langle L_\alpha \rangle$ and $\langle L_\beta \rangle$ are both sufficiently large so that the continuum step approximation can still be used, the analysis of Section 3 should still apply—at least up to Eq. (31), if the one or both interactions have different forms than that given by Eq. (1).

Perhaps a more severe problem is that the form of the interaction $V(L)$ can change: for Si(100) Alerhand et al. [24] showed that the leading contribution is a strain-derived repulsion proportional to $L^{-1} \ln(L/\pi a)$ in such situations. Such a potential would clearly complicate the solution from the

simple, elegant GWD. This issue is beyond the scope of the present work; we defer treatment to a later publication.

In fact, since the only interactions explicitly taken into account are between pairs of adjacent steps, our results clearly would also apply to TWDs of surfaces consisting of any number of types of steps, irrespective of the precise order in which these steps occur. Such a surface can be manufactured by cleaving a superlattice. Again, the interactions between neighboring steps would be the dominant consideration in determining the TWD for each terrace, although the pressure and compressibility, which are used to calculate $U(x_1, x_2)$, will depend on all of the interactions.

As a particularly instructive example, consider a cleaved surface in which several layers of material A alternate with several layers of material B. It might appear that the theory presented here would require all of the A-terraces to have the same TWD (and likewise all of the B-terraces), regardless of where they occur within the series. On the other hand, the elastic forces will clearly be different near the A–B transition than in the middle of the series of A-layers, due to the long-ranged elastic interactions. Clearly, the difference (which should be small) can only be accounted for by making $U(x_1, x_2)$ depend not only on the type of terrace and the types of neighboring steps, but also on other nearby terraces.

In conclusion, the approximations developed here should be broadly applicable to a wide range of stepped crystal surfaces, so long as the continuum step approximation remains valid.

Acknowledgement

Some of this work was supported by NSF-MRSEC at University of Maryland (NSF Grant No. DMR 00-80008).

References

- [1] H.-C. Jeong, E.D. Williams, Surf. Sci. Rep. 34 (1999) 179.
- [2] A. Zangwill, Physics at Surfaces, University Press, Cambridge, 1988.
- [3] D.M. Kolb, Surf. Sci. 500 (2002) 722.

- [4] G.A. Somorjai, M.A. Van Hove, *Prog. Surf. Sci.* 30 (1989) 201.
- [5] I. Makkonen, P. Salo, M. Alatalo, T.S. Rahman, *Surf. Sci.* 532–535 (2003) 154.
- [6] V. Shah, T. Li, K.L. Baumert, H. Cheng, D.S. Sholl, *Surf. Sci.* 537 (2003) 217.
- [7] G. Prévot, C. Cohen, D. Schmaus, P. Hecquet, B. Salanon, *Surf. Sci.* 506 (2002) 272.
- [8] F. Raouafi, C. Barreteau, M.C. Desjonquères, D. Spanjaard, *Surf. Sci.* 505 (2002) 183.
- [9] R. Heid, K.P. Bohnen, A. Kara, T.S. Rahman, *Phys. Rev. B* 65 (2002) 115405.
- [10] F. Starrost, E.A. Carter, *Surf. Sci.* 500 (2002) 323.
- [11] F. Rosei, R. Rosei, *Surf. Sci.* 500 (2002) 395.
- [12] S.V. Yanina, C.B. Carter, *Surf. Sci.* 513 (2002) L402.
- [13] H. Ibach, *Surf. Sci. Rep.* 29 (1997) 193.
- [14] N. Memmel, *Surf. Sci. Rep.* 32 (1998) 91.
- [15] R. Haight, *Surf. Sci. Rep.* 21 (1995) 275.
- [16] A.G. Naumovets, Z. Zhang, *Surf. Sci.* 500 (2002) 414.
- [17] K. Barnham, D. Vvedensky, *Low-Dimensional Semiconductor Structures: Fundamentals and Device Applications*, Cambridge University Press, Cambridge, 2001.
- [18] T.L. Einstein, in: W.N. Unertl (Ed.), *Physical Structure of Solid Surfaces*, I, North Holland, Amsterdam, 1996 (chapter 11).
- [19] N.C. Bartelt, T.L. Einstein, E.D. Williams, *Surf. Sci. Lett.* 240 (1990) L591.
- [20] H.L. Richards, S.D. Cohen, T.L. Einstein, M. Giesen, *Surf. Sci.* 453 (2000) 59.
- [21] N.C. Bartelt, T.L. Einstein, E.D. Williams, *Surf. Sci.* 276 (1992) 308.
- [22] Most of this material has been presented in J.A. Yancey, master's thesis, Texas A&M University-Commerce, unpublished.
- [23] K. Yagi, H. Minoda, M. Degawa, *Surf. Sci. Rep.* 43 (2001) 45.
- [24] O.L. Alerhand, A.N. Berker, J.D. Joannopoulos, D. Vanderbilt, R.J. Hamers, J.E. Demuth, *Phys. Rev. Lett.* 64 (1990) 2406.
- [25] R.P. Feynman, *Rev. Mod. Phys.* 20 (1948) 367.
- [26] M.E. Fisher, *J. Stat. Phys.* 34 (1984) 667.
- [27] P.-G. de Gennes, *J. Chem. Phys.* 48 (1968) 2257.
- [28] S.T. Chui, J.D. Weeks, *Phys. Rev. B* 23 (1981) 2438.
- [29] E.E. Gruber, W.W. Mullins, *J. Phys. Chem. Solids* 28 (1967) 875.
- [30] H. Gebremariam, S.D. Cohen, H.L. Richards, T.L. Einstein, *Phys. Rev. B* 69 (2004) 125404.
- [31] T. Ihle, C. Misbah, O. Pierre-Louis, *Phys. Rev. B* 58 (1998) 2289.
- [32] H.L. Richards, T.L. Einstein, *Phys. Rev. E* 72 (2005) 16124.
- [33] B. Joós, T.L. Einstein, N.C. Bartelt, *Phys. Rev. B* 43 (1991) 8153.
- [34] T. Guhr, A. Müller-Groeling, H.A. Weidenmüller, *Phys. Rep.* 299 (1998) 189.
- [35] F. Haake, *Quantum Signatures of Chaos*, second ed., Springer, Berlin, 1991.
- [36] T.L. Einstein, O. Pierre-Louis, *Surf. Sci.* 424 (1999) L299.
- [37] T.L. Einstein, H.L. Richards, S.D. Cohen, O. Pierre-Louis, *Surf. Sci.* 493 (2001) 460.
- [38] M. Giesen, T.L. Einstein, *Surf. Sci.* 449 (2000) 191.
- [39] O. Pierre-Louis, C. Misbah, *Phys. Rev. B* 58 (1998) 2259.
- [40] T. Ihle, C. Misbah, O. Pierre-Louis, *Phys. Rev. B* 58 (1998) 2289.
- [41] L. Barbier, L. Masson, J. Cousty, B. Salamon, *Surf. Sci.* 345 (1996) 197.
- [42] E. Le Goff, L. Barbier, L. Masson, B. Salamon, *Surf. Sci.* 432 (1999) 139.
- [43] E. Le Goff, L. Barbier, B. Salamon, *Surf. Sci.* 531 (2003) 337.
- [44] V. Privman, *Int. J. Modern Phys. C* 3 (1992) 857.
- [45] K. Blum, *Density Matrix Theory and Applications*, second ed., Plenum Press, New York, 1996.
- [46] M. Doi, S.F. Edwards, *The Theory of Polymer Dynamics*, Clarendon, Oxford, 1986.
- [47] K. Kremer, S.K. Sukumaran, R. Everaers, G.S. Grest, *Comp. Phys. Commun.* 169 (2005) 75.
- [48] R.K. Pathria, *Statistical Mechanics*, Butterworth Heinemann, Boston, 1996.
- [49] H. Goldstein, C. Poole, J. Safko, *Classical Mechanics*, third ed., Addison Wesley, San Francisco, 2002, p. 70.
- [50] N. Metropolis, A.R. Rosenbluth, M.N. Rosenbluth, A.H. Teller, E. Teller, *J. Chem. Phys.* 21 (1953) 1087.
- [51] M.E.J. Newman, G.T. Barkema, *Monte-Carlo Methods in Statistical Physics*, Oxford, New York, 1999.
- [52] B. Efron, *SIAM Rev.* 21 (1979) 460.
- [53] B.S. Swartzentruber, Y.-W. Mo, R. Kariotis, M. Lagally, M.B. Webb, *Phys. Rev. Lett.* 65 (1990) 1913.
- [54] H.J.W. Zandvliet, H.B. Elswijk, E.J. van Loenen, D. Dijkkamp, *Phys. Rev. B* 45 (1992) 5965.
- [55] N.C. Bartelt, R.M. Tromp, E.D. Williams, *Phys. Rev. Lett.* 73 (1994) 1656.
- [56] B.A.G. Kersten, H.J.W. Zandvliet, D.H.A. Blank, A. van Silfhout, *Surf. Sci.* 322 (1995) 1.